Eur. J. Biochem. **268**, 2083–2090 (2001) © FEBS 2001

Defined sequence segments of the small heat shock proteins HSP25 and αB-crystallin inhibit actin polymerization

Martin Wieske[1,*], Rainer Benndorf[1,2], Joachim Behlke[1], Rudolf Dölling[3], Gerlinde Grelle[1], Heinz Bielka[1] and Gudrun Lutsch[1]

[1]*Max Delbrück Center of Molecular Medicine, Berlin, Germany;* [2]*Department of Cell and Developmental Biology, University of Michigan Medical School, Ann Arbor, Michigan, USA;* [3]*Biosyntan GmbH, Berlin-Buch, Germany*

The interaction of small heat shock proteins (sHSPs) with the actin cytoskeleton has been described and some members of this family, e.g. chicken and murine HSP25 (HSP27), inhibit the polymerization of actin *in vitro*. To analyse the molecular basis of this interaction, we synthesized a set of overlapping peptides covering the complete sequence of murine HSP25 and tested the effect of these peptides on actin polymerization *in vitro* by fluorescence spectroscopy and electron microscopy. Two peptides comprising the sequences W43 to R57 (peptide 6) and I92 to N106 (peptide 11) of HSP25 were found to be potent inhibitors of actin polymerization. Phosphorylation of N-terminally extended peptide 11 at serine residues known to be phosphorylated *in vivo* resulted in decline of their inhibitory activity. Interestingly, peptides derived from the homologous peptide 11 sequence of murine αB-crystallin showed the same behaviour. The results suggest that both HSP25 and αB-crystallin have the potential to inhibit actin polymerization and that this activity is regulated by phosphorylation.

Keywords: actin polymerization; electron microscopy; fluorescence spectroscopy; small heat shock proteins; phosphorylation.

Heat shock and other environmental and pathophysiologic stresses stimulate the synthesis of heat shock proteins (HSPs). These proteins enable cells to survive and recover from stressful conditions by as yet incompletely understood mechanisms. Small heat shock proteins (sHSPs) constitute one of the major heat shock protein families and are characterized by a molecular mass of 15–40 kDa. They share a homologous sequence of about 90 amino acids, called the 'α-crystallin domain' because of its similarity with a sequence motif in the major eye lens protein αB-crystallin [1]. For sHSPs and αB-crystallin, which was also characterized as a sHSP [2], similar structural and functional properties have been described (reviewed in [3,4]). sHSPs and αB-crystallin have the ability to form multimeric complexes with a molecular mass of up to ≈ 800 kDa [5–8]. They occur in unphosphorylated and phosphorylated isoforms [9–13], and show chaperoning activity [14,15]. Furthermore, interactions with the cytoskeleton have been observed. For αB-crystallin interactions with actin and intermediate filament proteins have been described [16–21], while HSP25 appears to interact primarily with actin filaments [8,21–27]. (In this paper the sHSP of mouse, chicken and human is referred to as HSP25. Other names used for this protein are HSP27 or HSP28.) HSP25 from chicken, mouse and yeast has been identified as inhibitor of actin polymerization *in vitro* [8,22,23]. The unphosphorylated monomer is the active form in this process, whereas phosphorylated monomers and high molecular weight complexes are inactive [8]. Several of the studies cited above and others support the idea that an interaction of sHSPs with actin also occurs *in vivo*. Overexpression of HSP25 was shown to stabilize microfilaments against deleterious effects of hyperthermia and cytochalasin D in murine NIH/3T3 cells [24] and to increase the concentration of F-actin at the cell cortex and the pinocytotic activity in Chinese hamster cell lines [25]. HSP25 was found to colocalize, depending on the developmental stage, with the actin cytoskeleton in rat Sertoli cells [26] and with the I-band of myofibrils in cardiomyocytes of rat and human heart [21]. Furthermore, overexpression of HSP25 influenced the organization of cortical actin in bovine endothelial cell lines [27]. In several reports it was shown that the association of HSP25 with actin was modulated by phosphorylation of the protein [8,25,27–30]. As the microfilament network is an early target of cellular stress and different signal transduction pathways, it is likely that sHSPs may contribute to the regulation of actin dynamics under normal and stressful conditions.

To gain more information on the interaction between sHSPs and actin we tested a set of overlapping peptides derived from the murine HSP25 sequence [31] for their ability to inhibit actin polymerization. Two of the 22 HSP25-derived peptides studied were found to be potent inhibitors of actin polymerization *in vitro*. N-terminal extension and phosphorylation at serine residues of these peptides known to be phosphorylated *in vivo* modulated their inhibitory activity. A similar behaviour was observed for homologous peptides derived from the murine

Correspondence to G. Lutsch, Max Delbrück Center of Molecular Medicine, P.O.B. 740238, D-13092 Berlin-Buch, Germany.
Fax: + 49 30 9406 3814, Tel.: + 49 30 9406 3275,
E-mail: lutsch@mdc-berlin.de

Abbreviations: HSP, heat shock protein; sHSP, small heat shock protein.

**Present address*: Fritz Haber Institute of the Max Planck Society, 14195 Berlin, Germany.

(Received 19 October 2000, revised 16 January 2001, accepted 9 February 2001)

αB-crystallin sequence. The data elucidate for the first time part of the molecular mechanism underlying the interaction of HSP25 and αB-crystallin with actin.

EXPERIMENTAL PROCEDURES

Peptide synthesis

Peptides were synthesized by multiple solid phase peptide synthesis using the Fmoc chemistry procedure [32] on a PSSM-8 synthesizer (Shimadzu, Japan). Tentagel S RAM resin (RAPP Polymere GmbH, Germany) was used as carrier and 30% piperidine/dimethylformamide was used for Fmoc deprotection. All couplings were performed with *O*-(benzotriazol-1-yl)*N*,*N*′,*N*′-tetramethyluronium tetrafluoroborate/1-hydroxybenzotriazole/*N*-methylmorpholine in dimethylformamide. Fmoc-Ser(PO(Obzl)-OH (Novabiochem, Switzerland) was used for the synthesis of phosphoserine peptides. After synthesis all peptides were acetylated, cleaved from the resin by trifluoracetic acid and the resulting N-terminally acetylated peptide amides were analysed by HPLC and purified up to 85–95% purity. All peptides were characterized by MS using a MALDI I mass spectrometer (Kratos, Manchester, UK) [33]. After lyophilization peptides were stored at −20 °C. Before use, peptides were dissolved in distilled water, and concentrations were determined by quantitative amino acid analysis using a Sykam Analysator (Sykam, Gilching, Germany). Aliquots were used for determination of extinction coefficients of all peptides by recording of UV spectra.

Preparation of pyrene actin

F-actin was prepared from rabbit muscle powder according to the procedure of Pardee and Spudich [34] in buffer A (2 mM Tris/HCl pH 8.0, 0.2 mM $CaCl_2$, 0.2 mM Na_2ATP, 1 mM NaN_3). After extensive dialysis in buffer B (1 mM $NaHCO_3$ pH 7.6, 0.1 M KCl, 1 mM $MgCl_2$, 0.1 mM $CaCl_2$, 0.2 mM Na_2ATP, 1 mM NaN_3), the concentration of actin was adjusted to 1 mg·mL^{-1} using an extinction coefficient of 2.66×10^4·M^{-1}·cm^{-1} at 290 nm wavelength [35]. Labelling was overnight with a freshly prepared solution of *N*-(1-pyrene)iodoacetamide (Molecular Probes) as described by Kouyama and Mihashi [36]. Labelled F-actin was depolymerized by extensive dialysis against buffer C (2 mM imidazole/HCl pH 7.0, 0.1 mM $CaCl_2$, 0.2 mM Na_2ATP, 1 mM dithiothreitol, 1 mM NaN_3) and centrifuged for 2 h at 150 000 ***g*** in a Beckman TLA 100.3 rotor (Beckman Instruments) to obtain purified labelled G-actin in the supernatant.

Preparation of actin nuclei

Unlabelled F-actin was depolymerized by extensive dialysis against buffer C and separated from traces of F-actin by centrifugation for 2 h at 150 000 ***g*** in a Beckman TLA 100.3 rotor. Actin nuclei were prepared from the supernatant according to the procedure described by Pollard [35]. Briefly, 0.1 vol. of a 10 × buffer D solution (100 mM imidazole/HCl pH 7.0, 500 mM KCl) was added to unlabelled G-actin (1.5 mg·mL^{-1}), polymerized overnight, diluted to 0.5 mg·mL^{-1} with buffer D and equilibrated for at least 3 h before use in the polymerization assay.

Actin polymerization

Actin polymerization was measured by enhancement of fluorescence of pyrene-labelled actin using a Shimadzu RF5001PC spectrofluorometer (Shimadzu Europe GmbH, Duisburg, Germany) equipped with a 150-W Xenon lamp and a temperature-controlled sample compartment under control of the RF software (Shimadzu). Fluorescence was monitored at an excitation wavelength of 365 nm (5 nm slit) and an emission wavelength of 407 nm (10 nm slit) for 10 min at 25 °C. If not mentioned otherwise, assay mixtures were prepared directly in the cuvette (Hellma microcuvette, 3 mm light path) in a total volume of 60 μL in the following manner: 5 μL labelled G-actin (final concentration 2 μM) and different amounts of peptides in 5 μL distilled water were diluted into 44 μL buffer C and equilibrated for 3 min at 25 °C in the spectrofluorometer. To initialize polymerization, 1 μL actin nuclei and 5 μL of a salt solution (600 mM KCl, 24 mM $MgCl_2$) were added and thoroughly mixed. Recording was started within 10 s after addition of the latter. Under these conditions actin polymerization starts almost immediately and follows largely a linear kinetics up to 15 min. Addition of nuclei alone could not induce polymerization and addition of salt alone resulted in an extended lag period of about 5 min (Fig. 1A). For estimation of the stoichiometry of inhibition, slopes were determined from linear regression of the curves up to 5 min after start of the reaction, i.e. within the linear range of the slopes. They were calculated as percentage of inhibition of actin polymerization as compared to the control.

Electron microscopy

In this assay, conditions of polymerization were modified, in that nuclei were omitted in order to visualize only newly formed actin filaments. Furthermore, mixtures were incubated for 15 min before processing for electron microscopy because of the prolonged lag-period in the absence of actin nuclei (cf. Fig. 1A, curve 2). Samples were negatively stained with 1% uranyl formate using the double carbon film technique as described previously [7]. Micrographs were taken with an EM 910 electron microscope (LEO, Oberkochen, Germany) at 80 kV and a magnification of 50 000×.

RESULTS

Inhibition of actin polymerization by murine HSP25-derived peptides

To identify HSP25-derived fragments which interact with actin, a set of peptides was synthesized comprising the entire murine HSP25 sequence (Table 1). The size of the peptides ranged from 12 to 15 amino-acid residues with overlapping stretches of five to seven residues. These peptides were tested with respect to their ability to inhibit actin polymerization *in vitro* in a spectrofluorometric assay as described in Experimental procedures. When used at 20-fold molar excess over G-actin, only two peptides had an inhibitory effect on actin polymerization: peptide 6 (W43-R57) and peptide 11 (I92-N106). All other peptides had no influence under these conditions. The dependence of

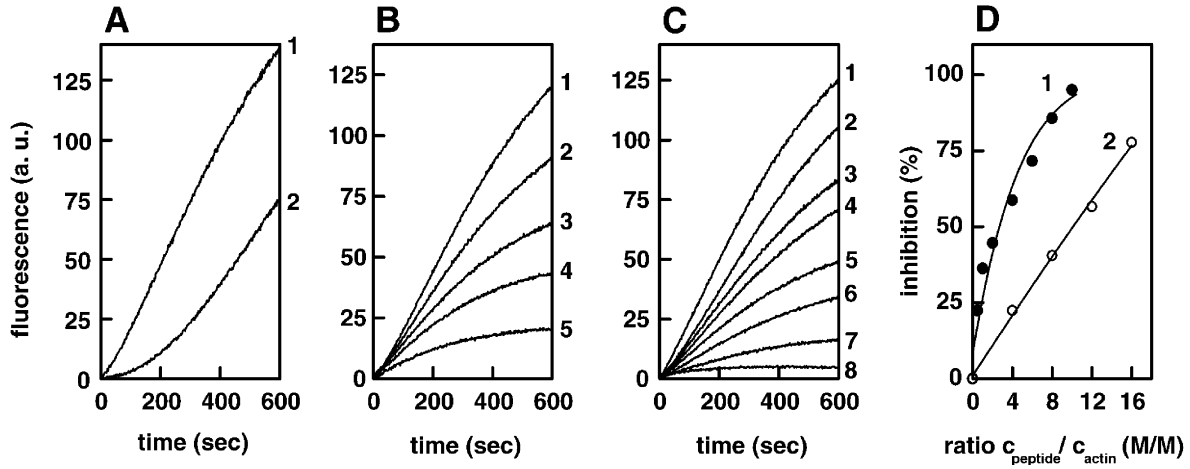

Fig. 1. Influence of HSP25 peptides on actin polymerization analysed by fluorescence spectroscopy. (A) Actin polymerization (1.2 μM G-actin) in the presence (curve 1) or absence (curve 2) of 0.1 μM actin nuclei. (B) Actin polymerization in the presence of 4-, 8-, 12- and 16-fold molar excess of peptide 6 over G-actin (2 μM) (curves 2–5, respectively; curve 1, control). (C) Actin polymerization in the presence of 0.5-, 1-, 2-, 4-, 6-, 8- and 10-fold molar excess of peptide 11 over G-actin (2 μM) (curves 2–8, respectively; curve 1, control). (D) Percentage of inhibition of actin polymerization at different molar ratios of peptide 6 (○) and peptide 11 (●) to G-actin estimated from the slopes of the curves during the first 5 min of polymerization. Values for peptides 6 and 11 are calculated from the curves shown in (B,C). Curves are representative of three to five independent experiments.

actin polymerization inhibition on the concentration of both peptides is demonstrated in Fig. 1B–D. Fig. 1B shows actin polymerization in the presence of varying amounts of peptide 6 (molar ratios of peptide 6 to G-actin 4 : 1, 8 : 1, 12 : 1, 16 : 1; curves 2–5, respectively) in comparison with the control without peptide 6 (curve 1). Fig. 1C shows a similar experiment for peptide 11 (molar ratios of peptide 11 to G-actin 0.5 : 1, 1 : 1, 2 : 1, 4 : 1, 6 : 1, 8 : 1, 10 : 1; curves 2–8, respectively) in comparison with the control without peptide 11 (curve 1). In Fig. 1D the percentage inhibition (compared with the controls) was calculated from

Table 1. Peptides derived from murine HSP25. Peptide 1 represents the N-terminus and peptide 22 the C terminus of HSP25. Peptides are synthesized as 15-mers with the exception of peptides no. 1, 2 and 10, and overlap by five to seven amino acids.

No	Residues	Sequence
1	1–12	MTERRVPFSLLR
2	7–18	PFSLLRSPSWEP
3	14–28	PSWEPFRDWYPAHSR
4	24–38	PAHSRLFDQAFGVPR
5	34–48	FGVPRLPDEWSQWFS
6	43–57	WSQWFSAAGWPGYVR
7	53–67	PGYVRPLPAATAEGP
8	63–77	TAEGPAAVTLAAPAF
9	73–87	AAPAFSRALNRQLSS
10	83–96	RQLSSGVSEIRQTA
11	92–106	IRQTADRWRVSLDVN
12	102–116	SLDVNHFAPEELTVK
13	112–126	ELTVKTKEGVVEITG
14	121–135	VVEITGKHEERQDEH
15	131–145	RQDEHGYISRCFTRK
16	140–154	RCFTRKYTLPPGVDP
17	150–164	PGVDPTLVSSSLSPE
18	160–174	SLSPEGTLTVEAPLP
19	169–183	VEAPLPKAVTQSAEI
20	177–191	VTQSAEITIPVTFEA
21	186–200	PVTFEARAQIGGPEA
22	195–209	IGGPEAGKSEQSGAK

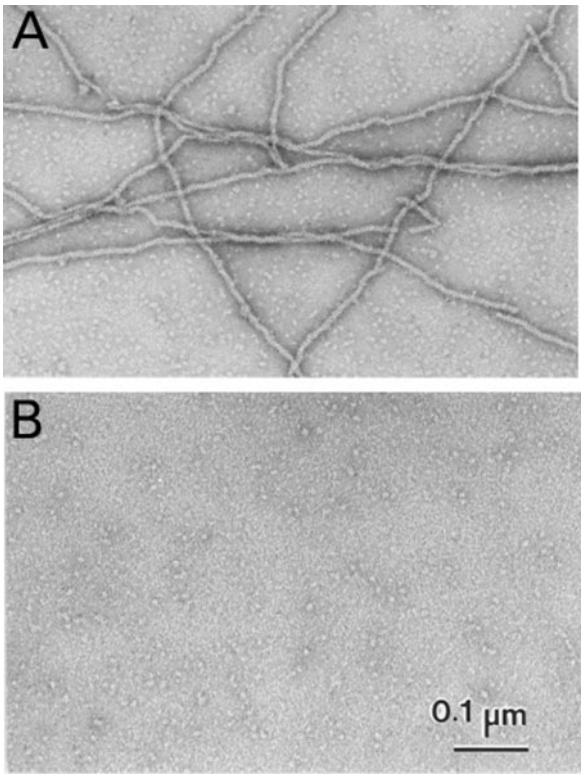

Fig. 2. Influence of murine HSP25 peptide 11 on actin polymerization analysed by electron microscopy. Actin polymerization (1.2 μM G-actin) in the absence (A) and in the presence of a 20-fold molar excess of peptide 11 (B).

Table 2. Compilation of various peptide 11-related sequences used in the actin polymerization assay. Peptides were derived from murine HSP25 and αB-crystallin sequences. A number of peptides was obtained by N- and C-terminal deletion and by N-terminal extension of peptide 11-related sequences (see also Fig. 3). Residue numbers indicate N- and C-terminal positions of the peptides in the amino-acid sequence of the protein. **S** indicates serines that are phosphorylated in the corresponding peptides (P). Activity of the peptides is related to that of the HSP25 peptide 11 which is set to 100% (see also Fig. 4). Numbers in parentheses refer to phosphorylated peptides.

Peptide	Residues	Sequence	Activity
11	92–106	IRQTADRWRVSLDVN	100
11αB	68–82	MRLEKDRFSVNLDVK	0
11c	–	TWLQRDANVRDISRV	0
11ΔN1	93–106	RQTADRWRVSLDVN	25
11ΔN2	94–106	QTADRWRVSLDVN	5
11ΔN3	95–106	TADRWRVSLDVN	0
11ΔN6	98–106	RWRVSLDVN	20
11ΔN9	101–106	VSLDVN	5
11ΔC4	92–102	IRQTADRWRVS	10
11ΔC6	92–100	IRQTADRWR	5
11ΔC8	92–98	IRQTADR	0
11ΔN4ΔC3	96–103	ADRWRVSL	0
11+N16(P)	76–106	AFSRALNRQL**S**SGVSEIRQTADRWRVSLDVN	50 (25)
11αB+N16(P)	53–82	SFLRAP**S**W-IDTGLSEMRLEKDRFSVNLDVK	50 (25)

the slopes of the curves obtained within 5 min of initializing the reaction. Curve 1 (peptide 11) and curve 2 (peptide 6) reveal that 50% inhibition of actin polymerization is achieved at peptide to G-actin ratios of 2.5 : 1 and 10 : 1, respectively.

To verify that the spectrofluorometric data reflect inhibition of formation of actin filaments, electron microscopic experiments were performed in parallel. As shown in control experiments without peptide (Fig. 2A), actin filaments of several micrometers length are loosely distributed in the G-actin background, whereas in the presence of a 10-fold molar excess of peptide 11 no actin filaments are observed (Fig. 2B). The same result was obtained when using a 20-fold molar excess of peptide 6 (not shown). Thus, the spectrofluorometric data are confirmed by electron microscopy.

Inhibition of actin polymerization by variants of murine HSP25-derived peptide 11

Further studies were performed with modifications of the most effective peptide 11 of murine HSP25. To analyse whether the amino acid composition of peptide 11, irrespective of the position of each amino-acid residue, or the specific position of each residue determines its interaction with actin, a scrambled control peptide (Table 2, peptide 11c) was synthesized. In designing this peptide, amino-acid residues known for their ability to participate in specific secondary structural elements were exchanged in their position. When using this peptide at 20-fold molar excess over G-actin, no effect on actin polymerization was observed (data not shown) indicating the specificity of the interaction of peptide 11 with actin.

In the following study, peptide 11 was modified by deleting amino-acid residues from both the N- and the C-terminus to identify residues involved in interaction with actin. Results of experiments carried out with these peptides in the actin polymerization assay are shown partially in Fig. 3A and summarized in Table 2 (abbreviations used for these peptides are also indicated in Table 2). Stepwise deletion of the first three amino-acid residues IRQ from the N-terminus of peptide 11 (peptides 11ΔN1, 11ΔN2, 11ΔN3) gradually reduced its activity to ≈ 25%, ≈ 5% and 0%, respectively (peptide 11ΔN3 see Fig. 3A, curve 2). Surprisingly, deletion of the first six amino-acid residues IRQTAD (peptide 11ΔN6) partially restored the inhibitory activity, resulting in ≈ 20% activity compared with peptide 11 (Fig. 3A, curve 6). The increased inhibitory activity of peptide 11ΔN6 compared to peptide 11ΔN3 suggests that the amino-acid residues TAD function as a linker between

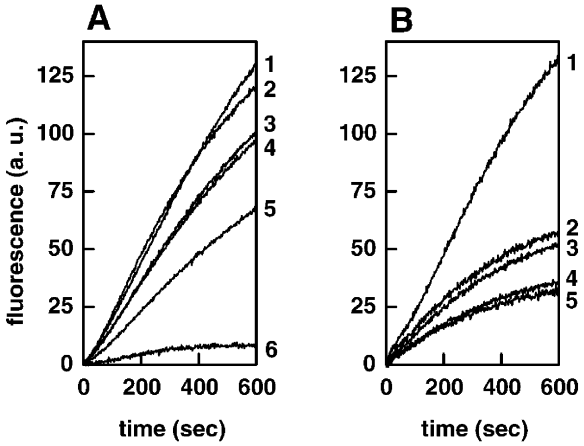

Fig. 3. Influence of various peptide 11 sequences on actin polymerization monitored by fluorescence spectroscopy. (A) Actin polymerization in the absence (curve 1) or presence of a 40-fold molar excess each of peptide 11ΔN3 (curve 2), 11ΔC6 (curve 3), 11ΔN9 (curve 4), 11ΔC4 (curve 5) and 11ΔN6 (curve 6) to G-actin. (B) Actin polymerization in the absence (curve 1) or presence of a 10-fold molar excess to G-actin each of peptide 11+N16P (curve 2), peptide 11αB+N16P (curve 3), peptide 11αB+N16 (curve 4) and peptide 11+N16 (curve 5). In each case 2 μM G-actin were used. Curves are representatives of three to five independent experiments.

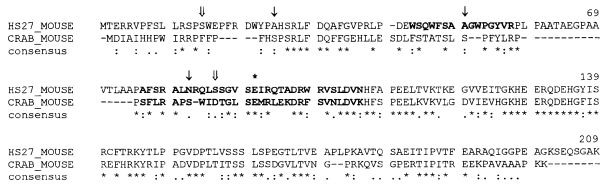

Fig. 4. Alignment of HSP25 and αB-crystallin sequences. Asterisks in the consensus line indicate identical amino-acid residues, colons indicate conserved substitutions and dots indicate semiconserved substitutions. Arrows indicate the phosphorylation sites of HSP25 (double arrow) and αB-crystallin (arrow). Sequences of peptide 6 and extended peptide 11 are shown in bold letters. The N-terminus of the α-crystallin domain is marked by an asterisk. Sequences are from murine HSP25 (GenBank Accession Number P14602) and murine αB-crystallin (GenBank Accession Number P23927).

two terminal motifs the coordination of which is necessary for an effective inhibition of actin polymerization (see Discussion). After deletion of the N-terminal amino-acid residues IRQ, this linker sequence seems to flex freely and thus to hinder sterically binding of peptide 11ΔN3, thereby reducing the inhibitory activity of the peptide in the actin polymerization assay. Deletion of the linker residues TAD from this peptide, however, resulted in improved binding and increased inhibitory activity. Further deletion from the N-terminus comprising the residues IRQTADRWR (peptide 11ΔN9) decreased the inhibitory activity to ≈5% compared with peptide 11 (Fig. 3A, curve 4). In comparison, deletion of amino-acid residues from the C-terminus of peptide 11 was slightly less effective in reducing the inhibitory activity of peptide 11. Deletion of the residues LDVN (peptide 11ΔC4) and VSLDVN (peptide 11ΔC6) reduced the inhibitory activity to ≈10% and ≈5%, respectively, of that of peptide 11 (Fig. 3A, curves 5 and 3). Further deletion from the C-terminus comprising the residues WRVSLDVN (peptide 11ΔC8) completely abolished the inhibitory activity of peptide 11. Also no inhibitory activity displayed a peptide where both the N- and the C-termini were deleted (11ΔN4ΔC3).

These data indicate that both the N-terminal (IRQ) and the C-terminal (WRVSLDVN) amino-acid residues of peptide 11 are involved in its inhibitory activity. For full activity, however, both the N- and the C-termini are required. That each terminus *per se* is not sufficient for an effective inhibitory activity is supported by the fact that the sequences IRQ and SLVDN are also included in the neighbouring peptides 10 and 12, which were inactive.

Because of the reported interaction of the closely related sHSP αB-crystallin with actin (see Introduction), an αB-crystallin-derived peptide corresponding to peptide 11 of HSP25 was synthesized (peptide 11αB). Its sequence was defined by sequence alignment of murine HSP25 and αB-crystallin as shown in Fig. 4. However, peptide 11αB had no effect on actin polymerization when used at 20-fold molar excess to actin and was inactive even at 40-fold molar excess (data not shown).

Phosphorylation affects the activity of HSP25- and αB-crystallin-derived peptides

Phosphorylation upon stress is one of the most prominent features of sHSPs, and it is known that phosphorylation of HSP25 modulates its effect on actin polymerization (see Discussion). To analyse the effect of phosphorylation on the actin polymerization inhibitory activity of HSP25- and αB-crystallin-derived peptides, we took advantage of the fact that some of the phosphorylation sites of these proteins are located N-terminally in close vicinity to peptide 11 (or the corresponding αB-crystallin-derived peptide; see Fig. 4). Therefore, the N-terminally extended HSP25-derived peptide (11+N16) as well as the αB-crystallin-derived peptide (11αB+N16) were synthesized. These peptides include known phosphorylation sites at S86 (murine HSP25 [11]); and S59 (murine αB-crystallin [9,13]); (see Table 2 and Fig. 4). From each peptide, the unphosphorylated as well as the phosphorylated form (11+N16P, 11αB+N16P) were synthesized. As shown in Fig. 3B, the unphosphorylated HSP25 peptide 11+N16 (curve 5) inhibited actin polymerization effectively at 10-fold molar excess over G-actin, with ≈50% of the inhibitory activity of peptide 11 (Table 2, cf. Fig. 1B). Reduced efficacy of peptide 11+N16 compared with peptide 11 may be due to higher flexibility of the N-terminal region of the molecule which may sterically hinder proper binding to actin (see Discussion). When the phosphorylated form of this peptide, 11+N16P, was used, the activity was reduced to ≈25% compared with peptide 11 (a 50% reduction in inhibitory activity compared with peptide 11+N16) (Fig. 3B, curve 2). Interestingly, in contrast with peptide 11αB, also the N-terminally extended form of the αB-crystalline peptide, 11αB+N16, demonstrated an inhibitory effect on actin polymerization (Fig. 3B, curve 4), which was comparable to the effect of the homologous HSP25-derived peptide (Table 2). Moreover, the activity was reduced when the phosphorylated form of this peptide, 11αB+N16P, was used (Fig. 3B, curve 3), the extent of reduction again being comparable to that of the homologous HSP25 peptide 11+N16P (Table 2). These data are remarkable in two aspects: (a) synthetic peptides derived from N-terminally extended peptide 11-like sequences of αB-crystallin inhibit actin polymerization *in vitro* like those of HSP25; and (b) phosphorylation of these peptides results in a reduction of their actin polymerization inhibitory activity. This behaviour is similar to that of intact native HSP25 (cf [8]).

DISCUSSION

This study provides the first evidence for a direct interaction of defined sequence segments of the small heat shock proteins HSP25 and αB-crystallin with actin thus specifying previous results about the function of HSP25 as inhibitor of actin polymerization [22] and implying a similar function for αB-crystallin. In particular, two regions of murine HSP25 have been identified which inhibit polymerization of actin effectively *in vitro*. Synthetic peptides comprising these sequences (peptides 6 and 11) inhibit actin polymerization half maximally at 10- and 2.5-fold molar excess over G-actin, respectively, compared with 0.1- to 0.2-fold molar excess of the isolated protein [8,22]. Thus, 10- to 100-fold higher amounts of the peptides are necessary to exert the same effects as the native protein. Similar relationships in inhibition of actin polymerization between actin-binding peptides and intact proteins have been described for other proteins: about 10-fold higher amounts of the actin-binding dodecapeptide of cofilin, an F-actin

side-binding and depolymerizing protein [37], and the actin-binding 30-residue fragment of thymosin β4, a G-actin sequestering protein [38], are necessary to achieve the same extent of inhibition as the intact protein. Lower efficacy of peptides compared with whole proteins may be due to the fact that peptides in general show a lower degree of higher ordered structure which may result in lower binding affinity, whereas in the whole protein these sequence segments are stabilized by neighbouring sequence elements and by interaction with other protein domains. The inhibitory effect of murine HSP25 peptide 11 on actin polymerization is ≈ 10-fold and threefold higher than that of the cofilin- [37] and thymosin β4-derived peptides [38]. Similarly, the inhibitory activity of murine HSP25 peptide 11 is about sixfold higher than that of a peptide (27-mer) derived from actin binding protein (ABP-120), an actin filament cross-linking protein of *Dictyostelium discoideum*, which displays 50% inhibition of actin polymerization at a 14-fold molar excess of the peptide over G-actin [39]. Furthermore, an actin-binding peptide (30-mer) derived from the N-terminus of actobindin from *Acanthamoeba castellani* was found to cause 50% inhibition of actin polymerization at about sevenfold molar excess of the peptide over G-actin [38], thus being three times less effective than the murine HSP25-derived peptide 11. Hence, HSP25-derived peptides 6 and 11 belong to the most active peptides inhibiting actin polymerization according to our knowledge.

Sequence comparison with actin-binding sites of other proteins reveals that no sequence homology exists between the HSP25-and αB-crystallin-derived peptides with actin polymerization inhibiting activity and the above-mentioned actin-binding dodecapeptide of cofilin and homologous sequences in the related proteins destrin, ADF and depactin [37]. Furthermore, no sequence similarity has been found to the actin-binding site of ABP-120, a conserved sequence which is also found in α-actinin, β-spectrin, dystrophin and fimbrin [39]. The same is true for the actin-binding sites of actobindin and thymosin β4 [38], the β subunit of CapZ [40] and proteins of the ezrin family [41]. Moreover, the actin-binding hexapeptide motif present in actobindin and thymosin β4 which also exists in a number of other actin-binding proteins like α-actinin, fimbrin, plastin, villin, myosin heavy chain and tropomyosin [42] is not found in HSP25 and αB-crystallin. Thus, sHSPs seem to represent a new family of actin-binding proteins. This interpretation is supported by recent results indicating that a further sHSP, rat HSP20, associates with actin [43].

The data about the inhibitory activity of HSP25-derived peptides can be correlated with data about the crystal structure of HSP16.5, a homologous sHSP from the archaebacterium *Methanococcus jannaschii* [44]. As evident from the crystal structure, the region homologous to peptide 11 of HSP25 is composed of two β strands in antiparallel orientation (β2, β3 in HSP16.5) connected by a turn of three amino-acid residues. Interestingly, this turn corresponds to residues TAD of murine peptide 11 proposed to act as a linker between the identified N- and C-terminal motifs involved in actin binding (see Results). It is very likely that this proposed linker sequence allows peptide 11 to adopt a conformation, which enables appropriate interaction with the actin molecule. Furthermore, it can be concluded from the crystal structure of Hsp16.5 that the region of the extended peptide 11 is most probably involved in intersubunit contacts in high molecular weight complexes of HSP25 as several of the amino-acid residues located in the homologous region of HSP16.5 (S31 to P61) contribute to contacts between subunits along the twofold axis of the complexes (see Kim *et al.* [44]). The region homologous to the HSP25-derived peptide 6, however, is missing from HSP16.5. According to the crystallographic data the N-terminus of HSP16.5 is located in the interior of the high molecular weight complexes, and it is likely that this also applies for the N-terminal region of HSP25. Thus, in high molecular weight complexes of HSP25 the amino-acid residues of peptides 6 and 11 are most probably buried and not accessible to interact with actin. In contrast, in HSP25 monomers these regions seem to be accessible and consequently they may interact with actin. This confirms previous results which indicated that only HSP25 monomers but not high molecular weight complexes of HSP25 inhibit actin polymerization *in vitro* [8].

Comparison of the inhibitory activity of peptides derived from homologous sequences of HSP25 and αB-crystallin showed a comparable extent of inhibition by the N-terminally extended peptides 11+N16. These data suggest that not only HSP25, but also αB-crystallin acts as an inhibitor of actin polymerization and that the activity of both proteins is at least partially mediated by these sequence segments. The lower efficacy of peptide 11+N16, compared with peptide 11, is likely to have the same causes as discussed above. Based on the crystal structure of HSP16.5 ([44], and see above), it can be concluded that the N-terminus of peptide 11+N16 contains a short β strand (β1) and is partially unstructured. As β1 belongs to another β sheet than β2 and β3 of peptide 11, it is very unlikely that peptide 11+N16 can adopt the correct tertiary structure present in the whole protein. Protection of binding sites and/or sterical hindrance by the flexible N-terminus of the 32-mer could result in lower efficacy of peptide 11+N16 compared with peptide 11. Differences in the inhibitory potential of the HSP25-derived peptide 11 and the αB-crystallin-derived peptide 11αB, on the other hand, may reflect cell-type specific mechanisms of regulation of the actin-binding ability of HSP25 and αB-crystallin which may occur through the interaction with different sHSP-binding proteins discovered recently [26,45]. Differential location of both proteins in rat and human heart [21] and rat kidney [46] supports this view.

Another interesting result described here is the reduced inhibitory activity of phosphorylated vs. unphosphorylated HSP25- and αB-crystallin peptides. This finding confirms previous results obtained with native murine HSP25 *in vitro* showing that unphosphorylated but not phosphorylated HSP25 monomers inhibit actin polymerization [8]. Furthermore, there is growing evidence about phosphorylation-dependent effects of HSP25 on the organization of microfilaments *in vivo*. Transfection or microinjection of different cell types with wild-type or nonphophorylatable HSP25 demonstrated, that only wild-type HSP25 protected the microfilament network against the deleterious effects of hyperthermia [24,30], cytochalasin D [24], free oxygen radicals [47] and cholecystokinin[48]. Protein phosphatase inhibitors and heat preconditioning were shown to prevent HSP25 dephosphorylation and F-actin disruption [29,49]. Pinocytosis activity [25], amount of membrane-associated F-actin [27] and cell migration [28] were shown to depend

on the presence of phosphorylatable HSP25. Obviously, phosphorylation of HSP25 is a prerequisite for rapid modulation of the actin cytoskeleton.

In comparison, data about interaction of αB-crystallin with actin are more rare. It was demonstrated previously that αB-crystallin colocalizes with microfilaments in cultured lens cells [50] and with the I-band of myofibrils in cardiomyocytes of rat and human heart [21]. Furthermore, αB-crystallin was found to bind to actin by affinity chromatography [16,17] and cosedimentation assays [17]. In addition, antisense experiments showed a disorganized microfilament network in cultured glial cells after reduction of αB-crystallin expression [19]. With respect to the influence of phosphorylation on the interaction of αB-crystallin with actin it was described that phosphorylated αB-crystallin was less effective in suppression of cytochalasin-induced depolymerization of actin filaments than the unphosphorylated form [20], in this respect αB-crystallin being comparable to HSP25. These findings are in accordance with our results on the interaction of αB-crystallin-derived peptides with actin and the regulation of their activity by phosphorylation. Interestingly, the different phosphorylation sites of αB-crystallin are phosphorylated by different kinases, and only S59, which is included in the extended peptide 11 tested in our assays, is phosphorylated by MAPKAP kinase-2 [51], which also phosphorylates the homologous phosphorylation site S86 in murine HSP25 [52]. Furthermore, it was shown that phosphorylation of αB-crystallin and HSP25 occurs in response to similar stressors in HeLa cells [53]. Obviously, in accordance with our *in vitro* results, regulation of the interaction of HSP25 and αB-crystallin with actin *in vivo* seems to occur through the same signal transduction cascade(s). Finally, it should be mentioned that regulation of activity by phosphorylation has also been observed for several other actin-binding proteins, e.g. synapsin [54], caldesmon [55], actin depolymerizing factor [56] and cofilin [57] which are unable to bind to actin in their phosphorylated states.

In conclusion, this work provides the first data about the molecular mechanism of the interaction of the small heat shock proteins HSP25 and αB-crystallin with actin. It describes actin-binding sites involved in inhibition of actin polymerization and provides data implying that the actin-polymerization inhibiting activity of both proteins is reduced by phosphorylation. Thus, HSP25 and αB-crystallin are characterized as actin-binding proteins the activity of which is regulated by phosphorylation, a feature that may also apply to other sHSPs.

ACKNOWLEDGEMENTS

The authors thank R. Kraft (Berlin) for support with amino acid analyses, E. Kotitschke (Berlin) for skilful technical assistance and R. R. Gilmont and R. F. Ransom (Ann Arbor) for critically reading the manuscript. This work was supported by grants of the Fond der Chemischen Industrie to H.B. and by grants of the Deutsche Forschungsgemeinschaft to R. B. (SFB 273, YE5; Be 1464/2-1) and G. L. (Lu 499/3-2).

REFERENCES

1. Ingolia, T.D. & Craig, E.A. (1982) Four small *Drosophila* heat shock proteins are related to each other and to mammalian α-crystallin. *Proc. Natl Acad. Sci. USA* **79**, 2360–2364.
2. Klemenz, R., Fröhli, E., Steiger, R.H., Schäfer, R. & Aoyama, A. (1991) αB-crystallin is a small heat shock protein. *Proc. Natl Acad. Sci. USA* **88**, 3652–3656.
3. Arrigo, P. & Landry, J. (1994) Expression and function of the low-molecular-weight heat shock proteins. In *The Biology of Heat Shock Proteins and Molecular Chaperones.* (Morimoto, R.I., Tissieres, A. & Georgopoulos, C., eds), pp. 335–373. Cold Spring Harbor Laboratory Press, Plainview, New York.
4. Ehrnsperger, M., Buchner, J. & Gaestel, M. (1997) Structure and function of small heat shock proteins. In *Molecular Chaperones in the Life Cycle of Proteins.* (Fink, A.I. & Goto, S., eds), pp. 533–576. Marcel Dekker Inc, New York.
5. Siezen, R.J., Bindels, J.G. & Hoenders, H.J. (1978) The quaternary structure of bovine α-crystallin. *Eur. J. Biochem.* **91**, 387–396.
6. Arrigo, A.P., Suhan, J.P. & Welch, W.J. (1988) Dynamic changes in the structure and intracellular locale of the mammalian low-molecular-weight heat shock protein. *Mol. Cell. Biol.* **8**, 5059–5071.
7. Behlke, J., Lutsch, G., Gaestel, M. & Bielka, H. (1991) Supramolecular structure of the recombinant small heat shock protein hsp25. *FEBS Lett.* **288**, 119–122.
8. Benndorf, R., Hayess, K., Ryazantsev, S., Wieske, M., Behlke, J. & Lutsch, G. (1994) Phosphorylation and supramolecular organization of murine small heat shock protein HSP25 abolish its actin polymerization-inhibiting activity. *J. Biol. Chem.* **269**, 20780–20784.
9. Chiesa, R., Gawinowicz Kolks, M.A., Kleiman, N.J. & Spector, A. (1987) The phosphorylation sites of the B_2 chain of bovine α-crystallin. *Biochem. Biophys. Res. Commun.* **144**, 1340–1347.
10. Voorter, C.E., de Haard Hoekman, W.A., Roersma, E.S., Meyer, H.E., Bloemendal, H. & de Jong, W.W. (1989) The *in vivo* phosphorylation sites of bovine αB-crystallin. *FEBS Lett.* **259**, 50–52.
11. Gaestel, M., Schröder, W., Benndorf, R., Lippmann, C., Buchner, K., Hucho, V.A., Erdmann, V. & Bielka, H. (1991) Identification of the phosphorylation sites of the murine small heat shock protein hsp25. *J. Biol. Chem.* **266**, 14721–14724.
12. Landry, J., Lambert, H., Zhou, M., Lavoie, J.N., Hickey, E., Weber, L.A. & Anderson, C.W. (1992) Human HSP27 is phosphorylated at serines 78 and 82 by heat shock and mitogen-activated kinases that recognize the same amino acid motif as S6 kinase II. *J. Biol. Chem.* **267**, 794–803.
13. Ito, H., Okamoto, K., Nakayama, H., Isobe, T. & Kato, K. (1997) Phosphorylation of αB-crystallin in response to various types of stress. *J. Biol. Chem.* **272**, 29934–29941.
14. Horwitz, J. (1992) α-Crystallin can function as a molecular chaperone. *Proc. Natl Acad. Sci. USA* **89**, 10449–10453.
15. Jakob, U., Gaestel, M., Engel, K. & Buchner, J. (1993) Small heat shock proteins are molecular chaperones. *J. Biol. Chem.* **268**, 1517–1520.
16. Chiesi, M., Longoni, S. & Limbruno, U. (1990) Cardiac alpha-crystallin. III. Involvement during heart ischemia. *Mol. Cell. Biochem.* **97**, 129–136.
17. Bennardini, F., Wrzosek, A. & Chiesi, M. (1992) αB-crystallin in cardiac tissue. Association with actin and desmin filaments. *Circ. Res.* **71**, 288–294.
18. Nicholl, I.D. & Quinlan, R.A. (1994) Chaperone activity of α-crystallins modulates intermediate filament assembly. *EMBO J.* **13**, 945–953.
19. Iwaki, T., Iwaki, A., Tateishi, J. & Goldman, J.E. (1994) Sense and antisense modification of glial αB-crystallin production results in alterations of stress fiber formation and thermoresistence. *J. Cell Biol.* **125**, 1385–1393.
20. Wang, K. & Spector, A. (1996) α-Crystallin stabilizes actin filaments and prevents cytochalasin-induced depolymerization in a phosphorylation-dependent manner. *Eur. J. Biochem.* **242**, 56–66.
21. Lutsch, G., Vetter, R., Offhauss, U., Wieske, M., Gröne, H.J., Klemenz, R., Schimke, I., Stahl, J. & Benndorf, R. (1997)

Abundance and location of the small heat shock proteins HSP25 and αB-crystallin in rat and human heart. *Circulation* **96**, 3466–3476.
22. Miron, T., Vancompernolle, K., Vandekerckhove, J., Wilchek, M. & Geiger, B. (1991) A 25-kD inhibitor of actin polymerization is a low molecular mass heat shock protein. *J. Cell Biol.* **114**, 255–261.
23. Rahman, D.R.J., Bentley, N.J. & Tuite, M.F. (1995) The *Saccharomyces cerevisiae* small heat shock protein Hsp26 inhibits actin polymerization. *Biochem. Soc. Trans.* **23**, 77S.
24. Lavoie, J.N., Gingras-Breton, G., Tanguay, R.M. & Landry, J. (1993) Induction of Chinese hamster HSP27 gene expression in mouse cells confers resistance to heat shock. HSP27 stabilization of the microfilament organization. *J. Biol. Chem.* **268**, 3420–3429.
25. Lavoie, J.N., Hickey, E., Weber, L.A. & Landry, J. (1993) Modulation of actin microfilament dynamics and fluid phase pinocytosis by phosphorylation of heat shock protein 27. *J. Biol. Chem.* **268**, 24210–24214.
26. Welsh, M.J., Wu, W., Parvinen, M. & Gilmont, R.R. (1996) Variation in expression of hsp27 messenger ribonucleic acid during the cycle of the seminiferous epithelium and co-localization of hsp27 and microfilaments in Sertoli cells of the rat. *Biol. Reprod.* **55**, 141–151.
27. Piotrowicz, R.S. & Levin, E.G. (1997) Basolateral membrane-associated 27-kDa heat shock protein and microfilament polymerization. *J. Biol. Chem.* **272**, 25920–25927.
28. Piotrowicz, R.S., Hickey, E. & Levin, E.G. (1998) Heat shock protein 27 kDa expression and phosphorylation regulates endothelial cell migration. *FASEB J.* **12**, 1481–1490.
29. Loktionova, S.A. & Kabakov, A.E. (1998) Protein phosphatase inhibitors and heat preconditioning prevent Hsp27 dephosphorylation, F-actin disruption and deterioration of morphology in ATP-depleted endothelial cells. *FEBS Lett.* **433**, 294–300.
30. Schneider, G.B., Hamano, H. & Cooper, L.F. (1998) In vivo evaluation of hsp27 as an inhibitor of actin polymerization: Hsp27 limits actin stress fiber and focal adhesion formation after heat shock. *J. Cell. Physiol.* **177**, 575–584.
31. Gaestel, M., Gross, B., Benndorf, R., Strauss, M., Schunck, W.-H., Kraft, R., Otto, A., Böhm, H., Stahl, J., Drabsch, H. & Bielka, H. (1989) Molecular cloning, sequencing and expression in *Escherichia coli* of the 25-kDa growth-related protein of Ehrlich ascites tumor and its homology to mammalian stress proteins. *Eur. J. Biochem.* **179**, 209–213.
32. Atherton, A. & Sheppard, R.C. (1989) *Solid Phase Peptide Synthesis – a Practical Approach.* IRL Press, Oxford.
33. Karas, M. & Hillenkamp, F. (1988) Laser desorption ionisation of proteins with molecular masses exceeding 10.000 daltons. *Anal. Chem.* **60**, 2299–2301.
34. Pardee, J.D. & Spudich, J.A. (1982) Purification of muscle actin. *Methods Enzymol.* **85**, 164–181.
35. Pollard, T.D. (1983) Measurement of rate constants for actin filament elongation in solution. *Anal. Biochem.* **134**, 406–412.
36. Kouyama, T. & Mihashi, K. (1981) Fluorimetry study of *N*-(1-pyrenyl) iodoacetamide-labelled F-actin. *Eur. J. Biochem.* **114**, 33–38.
37. Yonezawa, N., Nishida, E., Iida, K., Kumagai, H., Yahara, I. & Sakai, H. (1991) Inhibition of actin polymerization by a synthetic dodecapeptide patterned on the sequence around the actin-binding site of cofilin. *J. Biol. Chem.* **266**, 10485–10489.
38. Vancompernolle, K., Goethals, M., Huet, C., Louvard, D. & Vandekerckhove, J. (1992) G- to F-actin modulation by single amino acid substitution in the actin binding site of actobindin and thymosin beta 4. *EMBO J.* **11**, 4739–4746.
39. Bresnick, A.R., Janmey, P.A. & Condeelis, J. (1991) Evidence that a 27-residue sequence is the actin-binding site of ABP-120. *J. Biol. Chem.* **266**, 12989–12993.
40. Hug, C., Miller, T.M., Torres, M.A., Casella, J.F. & Cooper, J.A. (1992) Identification and characterization of an actin-binding site of CapZ. *J. Cell Biol.* **116**, 923–931.
41. Turunen, O., Sainio, M., Jääskeläinen, J., Carpen, O. & Vaheri, A. (1998) Structure-function relationships in the ezrin family and the effect of tumor-associated point mutations in neurofibromatosis 2 protein. *Biochim. Biophys. Acta* **1387**, 1–16.
42. Vancompernolle, K., Vandekerckhove, J., Bubb, M.R. & Korn, E.D. (1991) The interfaces of actin and *Acanthamoeba* actobindin. Identification of a new actin-binding motif. *J. Biol. Chem.* **266**, 15427–15431.
43. Brophy, C.M., Lamb, S. & Graham, A. (1999) The small heat shock-related protein-20 is an actin-associated protein. *J. Vasc. Surg.* **29**, 326–333.
44. Kim, K.K., Kim, R. & Kim, S.H. (1998) Crystal structure of a small heat-shock protein. *Nature (Lond.)* **394**, 595–599.
45. Welsh, M.J. & Gaestel, M. (1998) Small heat-shock protein family: function in health and disease. *Ann. NY Acad. Sci.* **851**, 28–35.
46. Smoyer, W.E., Ransom, R., Harris, R.C., Welsh, M.J., Lutsch, G. & Benndorf, R. (2000) Ischemic acute renal failure induces differential expression of small heat shock proteins. *J. Am. Soc. Nephrol.* **11**, 211–221.
47. Huot, J., Houle, F., Spitz, D.R. & Landry, J. (1996) HSP27 phosphorylation-mediated resistance against actin fragmentation and cell death induced by oxidative stress. *Cancer Res.* **56**, 273–279.
48. Schaefer, C., Clapp, P., Welsh, M.J., Benndorf, R. & Williams, J.A. (1999) HSP27 expression regulates CCK-induced changes of the actin cytoskeleton in CHO-CCK-A cells. *Am. J. Physiol.* **277**, C1032–C1043.
49. Loktionova, S.A., Ilyinskaya, O.P. & Kabakov, A.E. (1998) Early and delayed tolerance to simulated ischemia in heat-preconditioned endothelial cells: a role for HSP27. *Am. J. Physiol.* **275** (*Heart Circ. Physiol.* **44**), H2147–H2158.
50. Del Vecchio, P., MacElroy, K., Rosser, M. & Church, R. (1984) Association of α−crystallin with actin in cultured lens cells. *Curr. Eye Res.* **3**, 1213–1219.
51. Kato, K., Ito, H., Kamei, K., Inaguma, Y., Iwamoto, I. & Saga, S. (1998) Phosphorylation of αB-crystallin in mitotic cells and identification of enzymatic activities responsible for phosphorylation. *J. Biol. Chem.* **273**, 28346–28354.
52. Stokoe, D., Engel, K., Campbell, D.G., Cohen, P. & Gaestel, M. (1992) Identification of MAPKAP kinase 2 as a major enzyme responsible for the phosphorylation of the small heat shock proteins. *FEBS Lett.* **313**, 307–313.
53. Van den Ijssel, P.R.L.A., Overkamp, P., Bloemendal, H. & de Jong, W.W. (1998) Phosphorylation of αB-crystallin and HSP27 is induced by similar stressors in HeLa cells. *Biochem. Biophys. Res. Comm.* **247**, 518–523.
54. Bähler, M. & Greengard, P. (1987) Synapsin I bundles F-actin in a phosphorylation-dependent manner. *Nature (Lond.)* **326**, 704–707.
55. Yamashiro, S., Yamakita, Y., Ishikawa, R. & Matsumura, F. (1990) Mitosis-specific phosphorylation causes 83K non-muscle caldesmon to dissociate from microfilaments. *Nature (Lond.)* **344**, 675–678.
56. Agnew, B.J., Minamide, L.S. & Bamburg, R.J. (1995) Reactivation of phosphorylated actin depolymerizing factor and identification of the regulatory site. *J. Biol. Chem.* **270**, 17582–17587.
57. Moriyama, K., Iida, K. & Yahara, I. (1996) Phosphorylation of Ser-3 of cofilin regulates its essential function on actin. *Genes Cells* **1**, 73–86.